Hexagonal symmetry for smectic blue phases

B. Pansu and E. Grelet
Laboratoire de Physique des Solides, UMR 8502, Université Paris–Sud, F-91405 Orsay Cedex, France

M. H. Li
Institut Curie-Section de Recherche, URA 168, 11 rue Pierre et Marie Curie, F-75231 Paris Cedex 05, France

H. T. Nguyen
Centre de Recherche Paul Pascal, Avenue A. Schweitzer, F-33600 Pessac, France
(Received 6 October 1999; revised manuscript received 23 December 1999)

Smectic blue phases are liquid crystalline phases which exhibit both three-dimensional-orientational order and smectic positional order. X-ray scattering experiments reveal that at least one of these phases is not cubic, as classical blue phases, but offers a hexagonal symmetry. A comparison of the experimental patterns with the scattering patterns given by smectic double twist tubes sketched by Kamien is proposed.

PACS number(s): 61.30.Eb, 61.10.−i

I. INTRODUCTION

Liquid crystals offer a wide variety of phases with long range orientational order, but some phases like the smectic phases also exhibit additional quasi-long-range translational order. When the molecular mesogens are chiral, a spontaneous twist of the molecular orientation is observed. For instance, the classical nematic phase, which exhibits only a short range translational order, gives birth to the cholesteric phase [1] characterized by a one dimensional periodic orientational order with period or pitch much larger than the molecular sizes. At ''higher'' chirality, other phases called blue phases [2] appear in a temperature range located between the cholesteric phase and the isotropic one. Two of these blue phases, BP1 and BP2, exhibit a long range 3-dimensional orientational order, but classically only short range positional order. They show a cubic crystalline structure with selective Bragg reflections in the range or close to visible light. The monodomains are facetted and these phases appear with platelet textures under optical microscope. At ''low chirality,'' the BP1 and BP2 structures can be interpreted in terms of a 3D periodic director field. Twist extends not only in one direction like in the cholesteric phase but in both directions perpendicularly to the director. One can thus build ''double-twist'' cylinders whose size is determined by the tilt angle (θ) of the director at the surface with respect to the cylinder axis. The ''double twist'' cylinder radius is thus of the order of magnitude of the cholesteric pitch. The cubic structures (Fig. 1) can then be described by cubic networks of double-twist cylinders (with a surface tilt angle θ equal to 45°) separated by defect lines (disclination lines). In the ''high'' chirality limit, this description is no longer valid and a biaxial order parameter has to be introduced [3].

At lower temperatures smectic order may occur, but this translational order is not always compatible with the twist generated by the molecular chirality. For instance, the smectic layers in the Sm_A phase cannot be continuously twisted. Renn and Lubensky [4] predicted the existence of new phases called twist grain boundary phases, or TGB phases, which have been experimentally discovered in chiral thermotropic liquid crystals by Goodby *et al.* in 1989 [5]. Several TGB phases as TGB_A and TGB_C have already been identified [6–8]. These phases are usually observed upon cooling the isotropic phase (Iso) and an example of typical phase diagram is

$$\text{SmC*-TGB}_C\text{-TGB}_A\text{-Chol-BP-Iso.}$$

A twist-grain boundary phase is characterized by both smectic ordering and twist. In the SmC* phase, the layer normal is tilted compared to the director and parallel to the twist axis whereas, at least in the TGB_A phase, the twist axis is perpendicular to the layer normal. A continuous twist of the director in this direction is not compatible with smectic ordering. Renn and Lubensky have proposed a model where twist occurs between blocks or grains, of size l_b along the twist direction. Each block exhibits perfect smectic ordering (Fig. 2). The size of the blocks is intermediate between the smectic period (typically few nanometers) and the pitch (few hundred nanometers). Parallel screw dislocations lie in the walls between the grains.

Recently [9,10] a new sequence was discovered in a chiral material (called FH/FH/HH-18BTMHC) with the phase sequence

$$\text{SmC*-TGB phases-BP-Iso.}$$

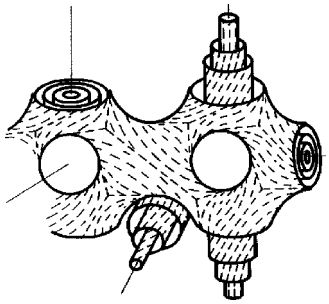

FIG. 1. Geometrical model of classical blue phases with 3D orientational order, but no long range positional order. Such models involve double twist tubes arrays and networks of disclination lines.

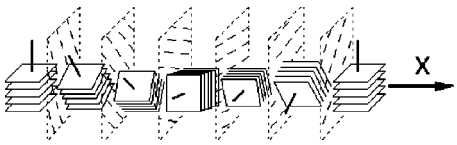

FIG. 2. Schematic representation of a twist grain boundary phase: smectic blocks are piled along the twist axis X. They are separated by twist boundaries made by walls of parallel screw dislocations.

Three blue phases have been observed in this compound: BP3 between 74.7 °C and 73.7 °C, BP2 between 73.7 °C and 73.3 °C, BP1 between 73.3 °C and 73.1 °C (upon cooling) [11]. The phase diagram has been established using calorimetric studies and optical microscopy. The pitch (about 0.2 μm) has been measured in the TGB_A phase using the Grandjean-Cano method. The textures of these blue phases are similar to those of classical blue phases and thus they have been labeled in the same way. However, in this phase diagram, there is no cholesteric phase between the blue phases and the TGB phases. X-ray scattering studies on this compound were reported in previous papers [12,13]. Such studies give informations on the order at the molecular level. By analyzing the width of the diffusion ring scattered by a powdered sample, we have shown that the smectic order already appears in the blue phases, but with a correlation length (typically 30 nm) smaller than in the TGB phase (typically 200 nm). One can notice that smectic order had been already detected in a metastable blue phase [14,15] in compounds exhibiting a direct blue phase to smectic transition. This phase has been called BP_S.

Using a well controlled oven, we succeeded in growing monodomains of smectic blue phases [13]. The scattering patterns performed on this monodomains exhibited four peaks indicating that the smectic order is not isotropic as one could expect for blue phases with short range smectic order, but more extended in some directions of the orientational cell. The correlation length associated with the peaks has been estimated to typically 70 nm. The experimental setup used at that time did not allow any rotation of the sample, thus preventing from any exploration of the whole reciprocal space. In order to perform this exploration, we have built an oven in which the capillary can rotate around its axis (the vertical axis). With this setup, we have grown up large monodomains of smectic blue phases and detected four pairs of smectic peaks exhibiting a hexagonal symmetry as detailed in the following section (II). This important result indicates that at least one of the smectic blue phase is not cubic, as confirmed by the observation of birefringence under optical microscope. Section III presents some computation of the scattering pattern of the smectic double twist tubes sketched

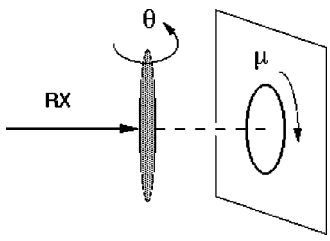

FIG. 3. Schematic representation of the scattering conditions.

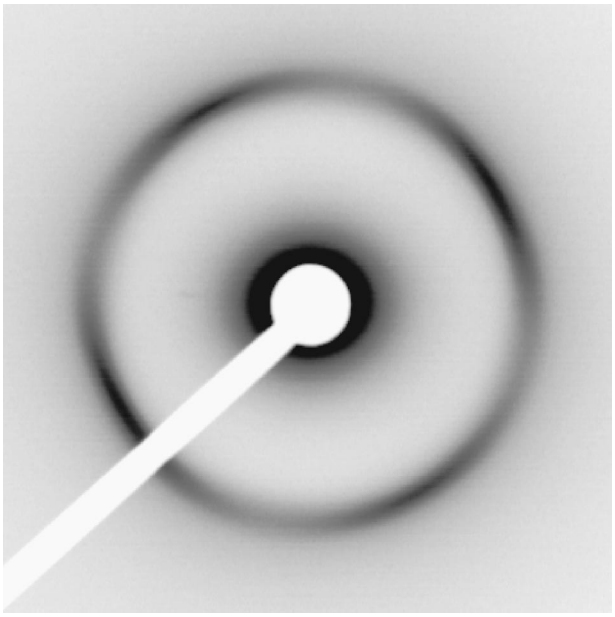

FIG. 4. Experimental scattering pattern obtained with temperature gradient close to 0.1 °C/mm at $\theta = -50°$. The P0 and P1 peaks are present.

by Kamien [19]. The comparison with the experimental patterns shows that this model must be revisited, at least the layers period distribution, to be fully compatible with our data.

II. EXPERIMENTAL EVIDENCE OF A HEXAGONAL SYMMETRY

In the setup we used in these experiments, the compound is contained in a glass capillary placed inside the hot stage whose description will be detailed in a forthcoming paper. The main features of this hot stage are its transparency to x

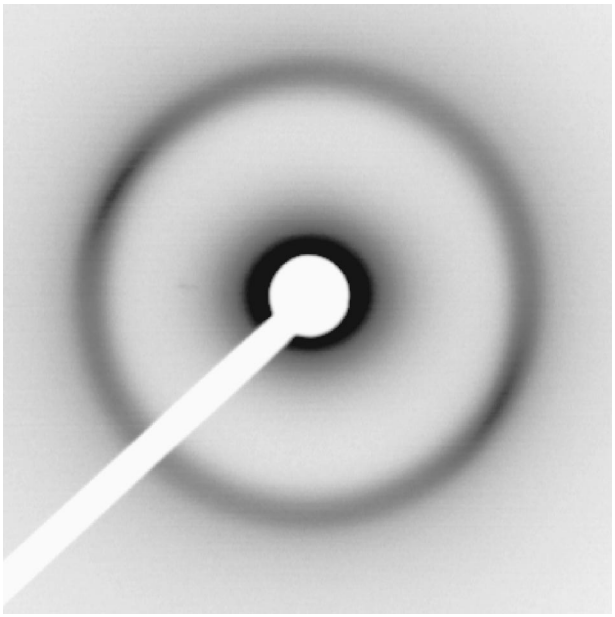

FIG. 5. Experimental scattering pattern obtained with temperature gradient close to 0.1 °C/mm at $\theta = 20°$. Only the P2 peak is observed.

TABLE I. Positions of the four peaks P0, P1, P2, P3 with temperature gradient 0.1 °C/mm (case a). μ is the angle with the vertical axis or with the temperature gradient. θ is the rotation angle around this axis. The monodomain has been grown with $\theta=0$ along the x-ray beam. The angles are given in degrees.

	P0	P1	P2	P3
θ	−49.5	−59	21	51.8
μ	59.4	−33	117	−112.4

ray with use of kapton and beryllium windows, a good stability in temperature (up to 0.01 °C) and the possibility of rotating the capillary around its main axis. Moreover, a slight vertical temperature gradient along the capillary can be applied in order to control the nucleation of the crystalline blue phases when cooling down [16]. We observe large monodomain growing for small cooling rate (typically 0.01 °C per 5 min). X-ray scattering experiments have been done in LURE (Orsay, France) using synchrotron radiation (beam size: 0.5×0.5 mm^2). After the monodomain has been grown up by a slow cooling down of the sample from the isotropic phase, different scattering patterns are recorded on imaging plates as long as the capillary is rotated by steps of 5°. Let us call θ this rotation angle (Fig. 3). For each value of θ we obtain a diffusion ring characteristic of the smectic order. This ring is not homogeneous and more intense in some directions as already observed (Figs. 4 and 5). The intensity $I(\theta,\mu)$ along the ring has been analyzed as a function of the angle with the vertical axis (μ). Then, by combining the various profiles, we can determine the position and the extension of the smectic peaks.

We have performed several series of experiments with two capillaries containing a small amount of FH/FH/HH-18BTMHC for two different temperature gradients (a: about 0.1 °C mm^{-1}; b: about 0.03 °C mm^{-1}). For low temperature decreasing rates, we have observed in the two cases (a and b) four pairs of peaks. In the following, each pair will be characterized by the position (θ,μ) of one of the peak, the angular coordinates of the second one being then $(\theta,\mu\pm180°)$. Among the four pairs of peaks, one pair is more intense and will be referred to as P0, the three other ones will be noted P1, P2, P3. The position of the peaks are shown in Tables I and II. From these values, we can deduce the angles between the directions along which the peaks are located. When two peaks are defined by the angles (θ_1,μ_1) and (θ_2,μ_2), the angle α between the two associated directions is

$$\cos\alpha=\sin\mu_1\sin\mu_2\cos(\theta_1-\theta_2)+\cos\mu_1\cos\mu_2. \tag{2.1}$$

TABLE II. Positions of the four peaks P0, P1, P2, P3 with temperature gradient 0.03 °C/mm (case b). The angles are given in degrees.

	P0	P1	P2	P3
θ	−24.4	−59.8	19.3	67.4
μ	−47	45.3	−128.1	94.9

TABLE III. Angles between the directions along which the peaks are observed (case a). The angles are given in degrees.

	P0	P1	P2	P3
P0	0	92	89	92
P1	92	0	118	120
P3	89	118	0	122
P4	92	120	122	0

Tables III and IV clearly show that the three directions along which P1, P2 and P3 are located are perpendicular to the direction along which the more intense peaks are located (P0). Moreover these directions are separated by angles close to 120°. This proves that there is a threefold axis in the structure and only one and that quasi-long-range smectic order is observed along this axis (P0) but also along three axes perpendicular to it (P1, P2, P3). At this point, it is important to notice that the Bragg scattering is not due to the periodicity of the orientational order and this for two reasons: the cell is too large to be detected with x-ray scattering (hundreds of nanometers) and it does not offer a density modulation but mainly an orientational order. X-ray scattering being sensitive to a density modulation, we detect the Fourier transform of some pattern in the cell linked to a periodicity of about 4 nm, that is the smectic order. Nevertheless, since the symmetry exhibited by these patterns is certainly correlated with the orientational order, these experimental results give information on the tridimensional cell. Therefore one can deduce that the smectic blue phase we have studied is *not cubic* as classical blue phase, *but hexagonal*. One can also notice that we do not observe any peak along the temperature gradient. The main peak P0 is quite always tilted at about 60° from the vertical axis, that is from the temperature gradient. Thus the orientation of the monodomains in the temperature gradient cannot be interpreted by symmetry arguments since no symmetry axis of the structure is aligned with the symmetry axis of the setup.

Phase diagram determined by calorimetric measurements show two blue phases, BP_{Sm1} and BP_{Sm2} in a temperature range of about 0.7 °C. Since BP_{Sm2} first appears when cooling down, we assume that the structure with a threefold symmetry we have determined is that of BP_{Sm2}. In the BP_{Sm1} temperature range (less than 0.2 °C), we no longer observe clear peaks, probably because it is hard to nucleate another crystalline phase when large monodomains of BP_{Sm2} have been grown [2,20]. In classical blue phases, BP2 and BP1 are cubic and it has been shown, for instance under electric field, that BP1 nucleates with a twofold axis parallel to a fourfold axis of BP2 [17]. Without external field, several orientations

TABLE IV. Angles between the directions along which the peaks are observed (case b). The angles are given in degrees.

	P0	P1	P2	P3
P0	0	93	90	92
P1	93	0	123	119
P3	90	123	0	118
P4	92	119	118	0

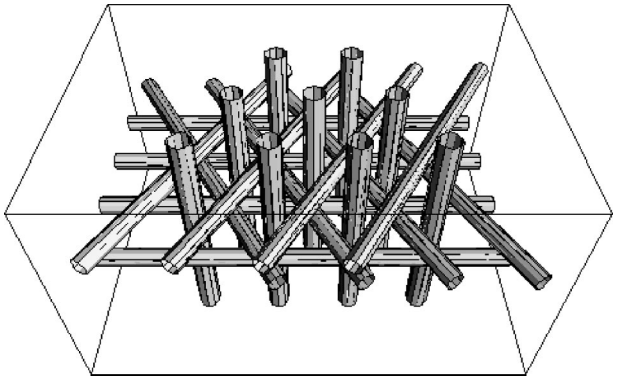

FIG. 6. Geometrical model of a 3D hexagonal blue phase based on an array of double twist tubes.

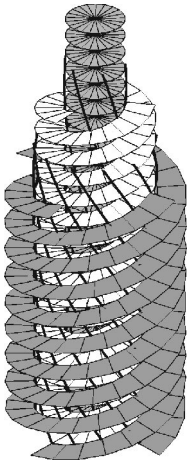

FIG. 7. Schematic representation of a smectic double twist tube (courtesy of Kamien).

of BP1 can be obtained from one BP2 monodomain. Under microscope, at the transition from classical BP2 to classical BP1 upon cooling, cross hatching appears in the BP2 monodomains indicating that each of these monodomains cannot generate a unique orientation of BP1 [20]. Single BP1 monodomains have been obtained by direct nucleation from the BP3 phase and never when the BP2 phase is present in the phase diagram. This seems to be the case also for smectic blue phases. To determine the structure of BP_{Sm1}, two ways are at present considered: either decreasing chirality by making eneantiomer mixtures, since BP_{Sm2} could disappear at lower chirality like classical BP2, or applying an electric field.

This evidence of a hexagonal symmetry proves that smectic blue phases are really new phases and not only classical blue phases with smectic fluctuations and that the smectic order deeply disturbs the orientational order. A three dimensional hexagonal structure has already been observed in classical blue phases but only under electric field [17]. A geometrical vision of a hexagonal blue phase in terms of double twist cylinders is given in Fig. 6. This structure is composed of a first set of parallel cylinders located on a hexagonal network. Three other sets of cylinders are perpendicular to the first one and pile up along a helicoidal axis (3_1 or 6_2). The experimental results obtained on BP_{Sm2} can be easily interpreted from this simple geometrical model by assuming that the regions where the smectic order can extend easily are the double twist cylinders cores. The P0 peaks correspond to the first set of cylinders, the P1, P2, P3 peaks correspond to the three other sets of cylinders. Such a geometrical model does not help to understand why the orientational order symmetry changes. Indeed the prediction of the phase diagram of classical blue phase requires sophisticated Landau theory [3,18]. Then the influence of the smectic order cannot be simply understood with use of geometrical model and the thermodynamic understanding of hexagonal smectic blue phases remains a challenge for theoreticians.

III. SMECTIC DOUBLE TWIST TUBES MODEL

A first approach for combining smectic order with three dimentional orientational order, as sketched in Fig. 7 has been proposed by Kamien [19]. As first pointed out in [13], the smectic order can extend easily in the core of the double twist tubes. Then, like in TGB structures, the rotation of the director is no longer continuous but involves annular grains. In order to respect the cylindrical symmetry, these grains cannot be filled up with perfect smectic layers. In the model proposed by Kamien, the layers build half-helicoids (generated by a half line and not a full straight line) wrapping around the main axis of the tube, except for the central core filled with a perfect smectic structure. The first annular grain corresponds to n_1 half-helicoids. The second one, as moving away from the core, corresponds to n_2 half-helicoids (n_2 greater than n_1) and so on. The boundary between two adjacent grain can be described by a wall of wrapping dislocation lines. Between the first annular grain and the core, there are n_1 dislocation lines. Between the first annular grain and the second one, there are (n_2-n_1) dislocation lines and so on. The smectic double twist tube of length L, as described by Kamien, is built by different annular grains. The core of radius R_1 is pure smectic with period d. Its contribution in the scattered intensity is a peak located at $\mathbf{q}=(0,0,2\pi/d)$ which extends over a distance $1/L$ in the z direction and $1/R_1$ in the radial directions. Then one encounters different annular grains with increasing values of the number n of helicoids increasing more rapidly that the radii limiting the grains. The main characteristic of each annular grain is the number n of half helicoids which build it, the period a of each helicoid, the minimum radius R_1 and the maximum radius R_2. At a distance r from the main axis, the distance $d(r)$ between smectic layers along the layer normal and the tilt angle $\theta(r)$ of the director and the layer normal with respect to the tube axis are given by

$$d(r)=\frac{a}{n}\cos\theta(r), \tag{3.1}$$

$$\tan\theta(r)=\frac{a}{2\pi r}. \tag{3.2}$$

From these equations, one can see that the tilt angle decreases with increasing r although there is no twist inside each grain (Appendix A). The distance between the smectic layers increases with increasing r, which implies some con-

tribution to the elastic energy. The boundary condition between two grains, noted 1 and 2 are at the boundary ($r=R$):

$$d_1(R)=d_2(R), \tag{3.3}$$

$$\theta_2(R)=\theta_1(R)+\Delta\theta. \tag{3.4}$$

The number of dislocations at the boundary between the two grains is just given by $N=n_2-n_1$. The whole determination of the smectic double twist tube configuration, that is all the characteristics of the grains, implies a generalization of the approach of Renn and Lubensky for the TGB phase. In their model, a simple argument can give the grain size (Fig. 2). If the screw dislocations within each grain boundary are separated by a distance l_d, then the rotation angle of adjacent blocks is given by $\Delta\theta=d/l_d$ where d is the smectic period (for small angles). The size of the blocks l_b is also linked to $\Delta\theta$, the rotation angle between two adjacent grains, through the relation: $\Delta\theta/2\pi=l_b/p$ where p is the twist period. Therefore the two lengths l_b, the size of the blocks, and l_d, the distance between the screw dislocations, are related to d and p via $l_d l_b=dp/2\pi$. A reasonable estimation of the size of the blocks can be obtained by taking $l_b=l_d=\sqrt{dp/2\pi}$. Thus the size of the blocks in the TGB phase is intermediate between the smectic period (typically few nanometers) and the pitch (few hundred nanometers). The extension of the TGB model to the smectic double twist tube configuration has not yet been done and the cylindrical symmetry does not allow a simple estimation of the size of the grains. Then we have chosen arbitrarily one configuration to sketch the main features of the Fourier transform of a smectic double twist tube. The smectic double twist configuration we have chosen is composed of five grains (Appendix B). The main characteristics of its architecture are as follows: the width of the grains is nearly the same, the twist angle at each boundary is close to 10°, as the one measured on TGB_A phase, the intensity scattered by each grain is roughly the same for all the grains. In this configuration, the distances between the screw dislocations inside the boundaries are comparable with the width of the grains. In the classical model of blue phases, the radius of the double twist tube is imposed by the kissing conditions between perpendicular tubes and the tilt angle at the surface of the tubes is 45°. In the model sketched by Kamien, this kissing condition imposes some vanishing of the smectic order in between the tubes and therefore the tilt angle of the director at the surface of the smectic double twist tube cannot be determined only by geometrical estimations, energetical considerations are also required.

The scattering pattern of such a configuration is sketched on Fig. 8. It has been computed as sketched in Appendix C. The circle drawn on this figure is related to the period of the smectic core. The intensity scattered by each annular grain is located on a ring whose intersection with the (q_x,q_y) plane consists on two segments as drawn in Fig. 8. Therefore the whole scattering pattern looks like a discontinuous arc. Its extension roughly corresponds to the director orientation at the external surface of the double twist tube. Figure 8 has been drawn using the approximation of infinite double twist tubes. In that case, the intensity is located at a precise value of $q_z=q_o$. For the variation of the intensity upon q_x, one

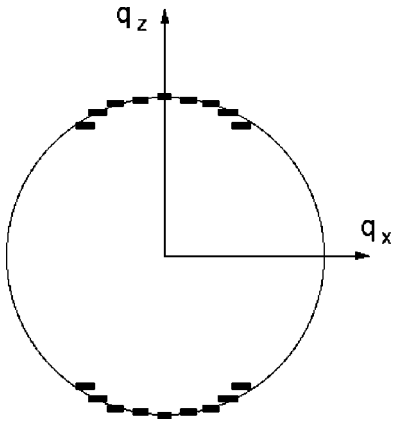

FIG. 8. Schematic representation of the Fourier transform of a smectic double twist tube. The circle is related to a constant smectic period.

can introduce the Bessel function of order n in the Fourier transform of a set of n helicoids in the computation of the factor structure of the tubes. The scattered intensity thus exhibits some maximum in the q_x direction depending on the number of helicoids inside the grain and on the limiting radii of the grain . In our case, the smectic order is not long range order. Numerical computations have shown that the maximum of intensity is shifted towards larger q_x for q_z larger than q_o and lower q_x for q_z lower than q_o. Therefore the segments are deformed but they mean position remains the same. The following conclusions thus remain valid even for finite range smectic order. In Fig. 8, one can see that the ring on which is located the scattered intensity is close to the circle which corresponds to a powder of perfect smectic domains, but it is also obvious that it deviates from it for the last grains. This is due to the regular increase of the smectic period that is intrinsically present in the model. Indeed the smectic period increases with r, the distance to the main axis, inside a grain and this period is continuous at the boundary between two adjacent grains. The increase of the smectic period in the direct space thus appears as a shift of the maximum intensity towards lower values of q in the reciprocal space.

The experimental patterns $I(Q,\mu,\theta)$ where Q is the scattering vector modulus, μ the angle with the vertical axis and θ the rotation angle around the vertical axis, exhibit for given θ intense arcs but without any discontinuity. This can be easily explained by the fact that the scattering volume (about 0.25 mm^3) contains more than 10^{10} hexagonal cells if one assumes that the monodomain fills the capillary. Then there are certainly statistical and thermal fluctuations of both the orientation and the configuration of the smectic double twist tubes. The continuous arc that is experimentally observed can be seen as some average of discontinuous arcs over some disorientation. To get more information from the experimental patterns, and particularly on the variation of the smectic period, we have performed a detailed analysis of the peak profiles. For each peak, we have taken the scattering pattern performed for the angle θ as close as possible as those indicated in Table I. Then we have measured the extension of the experimental intense arc for the different peaks. The FWHM (full width at height medium) of the intensity along the arc (integrated over its width) is typically around $\Delta\mu=40°$ for

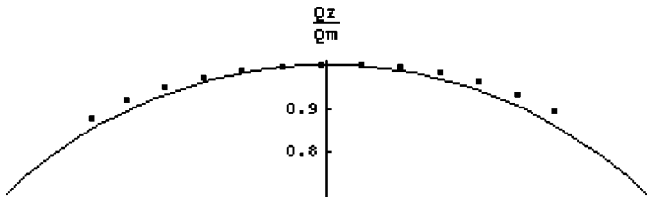

FIG. 9. Analysis of the profile of the P0 peak (Table I). The dots indicate the location Q_m of the maximum intensity along the radial direction. Q_o is the value of Q_m at the absolute maximum. $Q_m/Q_o=1$ corresponds to a constant smectic period (circle of Fig. 8).

the P0 peak and around $\Delta\mu=30°$ for the P1, P2, P3 peaks. The P0 peak is the more intense and more extended than the three other ones. We have also explored the radial width of the P0 peak ($\theta=50°$). For each value of μ around the main value $\mu=59.4°$, we have determined the position of the maxima of the scattered intensity $Q_m(\mu)$ and the value of the FWHM. The results are shown in Figs. 9 and 10. It is clear that the location of the maxima moves towards larger values of Q and not towards smaller ones as expected, in the model proposed by Kamien, when moving away from $\mu(P0)=59.4°$. They are located in between a perfect circle of radius Q_o, the value of Q at the absolute maximum, and a straight line (full line in 9). The radial width of the peak (ΔQ) increases when moving away from the central position ($\mu=59.4°$). It seems non-symmetrical but this effect could be due to the beam shape: the horizontal focus of the beam and the vertical one are not identical.

Nevertheless, even taking into account some fluctations in the model of smectic double twist tube, one should observe the shift of the location of the maximum intensity along the radial direction of the reciprocal space towards lower values of Q and not larger ones. This is not what we observe experimentally. The real smectic double twist tube configuration could be different from the considered one. Nevertheless, the increase of the smectic period should be revealed by the scattering pattern. This means that the behavior of the distance between the layers could be not correctly described in the model of Kamien. We have also verified that the experimental patterns cannot be explained by a simple model involving only smectic cores without any helicoid with finite

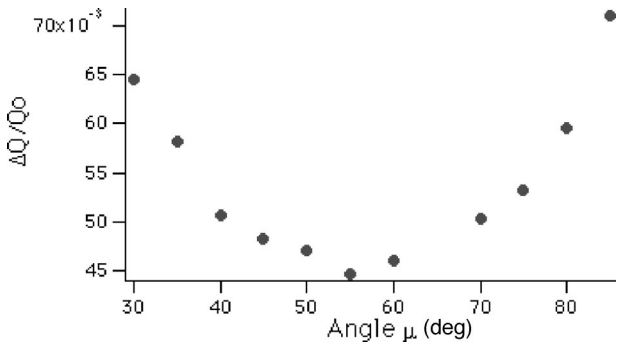

FIG. 10. Analysis of the profile of the P0 peak (Table I). The dots indicate the width of the peak (full width at height medium) along the radial direction as a function of the angle μ (in degrees). It slightly increases when moving away from the absolute maximum.

extension and fluctuating orientation. Therefore to explain our experimental observations, two ways can be investigated. The first one consists in revisiting the boundary condition on the smectic period in the model of Kamien. Intoducing some edge component in the dislocations would allow for a jump in the smectic period when going from one grain to the other. That means that the dislocations could not be pure screw ones but could also have an edge component. Therefore the mean smectic period could be the same inside all the grains as the smectic period in the core. One can then wonder how the scattering pattern would be modified. The second way of investigation would be considering some tilt of the molecules inside the layers that is some SmC feature occuring.

IV. CONCLUDING REMARKS

These experiments clearly show that smectic blue phases are really original phases since at least one of them is not cubic as classical blue phases, but exhibits a hexagonal symmetry. This symmetry has been detected on the smectic order and not yet on the orientational cell. The determination of the symmetry of the other smectic blue phase is in progress. We do not yet understand why the smectic order so much disturbs the tridimensional order changing the cubic symmetry into a hexagonal one. A full understanding of the phase diagramm probably requires both sophisticated Landau theory as for classical blue phases and physics of defects as for TGB phases. This remains a great challenge for theoreticians.

ACKNOWLEDGMENTS

We have much appreciated the kindness and the efficiency of D. Dallé who has designed and built the oven we have used. We thank J. Doucet and D. Durand from LURE for their hospitality and their competence.

APPENDIX A: NO TWIST FOR THE NORMAL TO AN HELICOID

Although an helicoid is a chiral architecture, the normal to its surface does not twist. From a more general point of view, a normal to any surface cannot twist. Indeed let us consider a family of surfaces determined by the following equation:

$$f(x,y,z)=C. \tag{A1}$$

The normal $\mathbf{n}$ is just given by

$$\mathbf{n}=\frac{\nabla f}{|\nabla f|}. \tag{A2}$$

Then

$$\nabla\wedge\mathbf{n}=\nabla\frac{1}{|\nabla f|}\wedge\nabla f \tag{A3}$$

and therefore

$$(\nabla\wedge\mathbf{n})\cdot\mathbf{n}=0. \tag{A4}$$

This last equation indicates that the normal to a surface cannot twist. This is also true for an helicoidal surface even if

TABLE V. Arbitrary parameters describing the smectic double twist tube configuration used in the computation of the Fourier transform.

Grain	n	R_1	R_2	a	a/n	$\theta(R_1)$	$\theta(R_2)$	$d(R_1)$	$d(R_2)$
Central grain	0	11 nm			0°	0°	4 nm	4 nm	
Grain I	3	11.5 nm	22 nm	12.169 nm	4.056 nm	9.56°	5.03°	4 nm	4.04 nm
Grain II	9	22 nm	32 nm	37.694 nm	4.16 nm	15.25°	10.62°	4.04 nm	4.116 m
Grain III	18	32 nm	41 nm	79.71 nm	4.43 nm	21.63°	17.19°	4.116 nm	4.23 nm
Grain IV	27	41 nm	49 nm	127.43 nm	4.72 nm	26.32°	22.48°	4.23 nm	4.36 nm

this surface is chiral, that is non-identical to its mirror image. In that case, this can be seen directly on the expressions of the normal components in cylindrical coordinates (r,ϕ,z):

$$n_r = 0, \tag{A5}$$

$$n_\phi = -\sin\theta, \tag{A6}$$

$$n_z = \cos\theta. \tag{A7}$$

Then $\nabla \wedge \mathbf{n}$ has two nonvanishing components:

$$(\nabla \wedge \mathbf{n})_\phi = \sin\theta \frac{\partial\theta}{\partial\theta}, \tag{A8}$$

$$(\nabla \wedge \mathbf{n})_z = \frac{\sin\theta}{r} - \cos\theta \frac{\partial\theta}{\partial r}. \tag{A9}$$

Therefore,

$$\mathbf{n}\cdot(\nabla \wedge \mathbf{n}) = -\frac{\partial\theta}{\partial r} + \frac{\sin\theta\cos\theta}{r}. \tag{A10}$$

Using $\tan\theta(r) = a/2\pi r$, one can easily show that $\mathbf{n}\cdot(\nabla \wedge \mathbf{n}) = 0$. Therefore, even if θ varies as a function of r, the normal to the helicoid does not twist.

APPENDIX B: CONSTRUCTION OF A DOUBLE TWIST TUBE CONFIGURATION

Let us first recall the relationship between the various parameters in an annular grain composed of n helicoidal sheets. a is the period of each helicoid and its equation is in cylindrical coordinates r,ϕ,z is

$$\phi = 2\pi\frac{z}{a} = q_a z. \tag{B1}$$

The normal to the helicoid which in our case is parallel to the director (SmA case) is

$$n_r = 0, \tag{B2}$$

$$n_\phi = -\sin\theta, \tag{B3}$$

$$n_z = \cos\theta. \tag{B4}$$

At the distance r from the main axis, θ is given by

$$\tan\theta = \frac{a}{2\pi r} \tag{B5}$$

and the distance d between the layers, which is the smectic period, is

$$d(r) = \frac{2\pi r\sin\theta}{n}. \tag{B6}$$

At the boundary between two annular grains, relationships between the various parameters can be deduced from the variation of the tilt angle θ and the smectic period d. In the model proposed by Kamien, the smectic period is continuous through the boundary. The tilt angle is discontinuous since it is a twist boundary. The twist angle will be called $\Delta\theta$. In the following equations, indexes 1 and 2 will be related to the two sides of the boundary located at the distance R from the main axis. At the boundary, all the following equations must be verified:

$$\theta_2 = \theta_1 + \Delta\theta, \tag{B7}$$

$$\tan\theta_1 = \frac{a_1}{2\pi R}, \tag{B8}$$

$$\tan\theta_2 = \frac{a_2}{2\pi R}, \tag{B9}$$

$$\frac{\sin\theta_1}{n_1} = \frac{\sin\theta_2}{n_2}. \tag{B10}$$

We have built a smectic double twist tube following these rules. We have imposed a twist angle $\Delta\theta$ close to 10° and we have chosen the radii such as the intensity scattered by each grain is nearly the same for all the grains. The characteristics of the smectic double twist tube we have used to compute the scattered intensity profile are listed in Table V.

APPENDIX C: FOURIER TRANSFORM OF AN ANNULAR GRAIN COMPOSED OF *N* HELICOIDAL SHEETS

Let us consider an annular grain composed of n half helicoids of period a with regular spacing. The equation of a half helicoid in cylindrical coordinates r,ϕ,z is

$$\phi = 2\pi\frac{z}{a} = q_a z, \tag{C1}$$

where a is the period of each helicoid along the tube axis. The grain extends over a radius range: $R_1 < r < R_2$. Let us call L the length of the tube which corresponds to the range of the smectic order. Along the grain axis, this architecture is periodic with a period a_o equal to a/n and close to the smec-

tic period. The pattern which reproduces upon the period a_o is just one turn of one helicoid. Due to this periodicity, the intensity along this axis will be located around discrete values of q_z, that is $q_z = pq_o$ where $q_o = 2\pi/a_o$ and p is an integer. In our experiments, we only see the first order peak $p=1$ close to $2\pi/d$ where d is the smectic period. The width of this peak along the z axis is linked to the extension of the smectic order in this direction and varies as $2\pi/L$. In a previous experimental paper, it has been estimated to about 70 nm [13]. Due to the symmetry around the grain axis, the scattered intensity must be invariant under rotation around this main axis. Its variation upon q_1, the distance to the grain axis in the reciprocal space, then depends on the structure factor of one turn of helicoid. Therefore the whole structure factor $A(\mathbf{q})$ of the annular grain with n half helicoids for a scattering vector $\mathbf{q}=(q_1,0,q_z)$ in the x,z plane, is given by

$$A(\mathbf{q}) = \sum_{k=1}^{m} \exp^{iq_z k a_o} \int_0^a dz \int_{R_1}^{R_2} dr \sqrt{1+q_a^2 r^2} \times \exp^{iq_1 r \cos(q_a z)} \exp^{iq_z z}, \tag{C2}$$

where m is the total number of turns of helicoids over the distance L and $dzdr\sqrt{1+q_a^2r^2}$ the elementary area of each helicoid. For $q_z = q_o$ (first order, $p=1$), the scattered amplitude along the radial direction is then given by

$$A(q_1,q_o) = nm \int_{R_1}^{R_2} dr \sqrt{1+q_a^2 r^2} \int_0^a dz \exp^{iq_1 r \cos(q_a z)} \exp^{iq_o z}. \tag{C3}$$

The last integral involves Bessel function of order n

$$\int_0^a dz \exp^{iq_1 r \cos(q_a z)} \exp^{iq_o z} = q_o^{-1} J_n(q_1 r). \tag{C4}$$

The Bessel function $J_n(x)$ presents some maximum for increasing values of x with increasing n. Therefore the intensity scattered by one annular grain will be maximum for

$$q_z = q_o \pm \sim 2\pi/L \tag{C5}$$

and

$$q_1 \sim \frac{\max(J_n)}{R}. \tag{C6}$$

where $\max(J_n)$ is the position of the first maximum of the Bessel function of order n and R is the mean value of the annular grain radius.

[1] P.G de Gennes and J. Prost, *The Physics of Liquid Crystals* (Clarendon Press, Oxford, 1993).
[2] H. Stegemeyer, Th. Blumel, K. Hiltrop, H. Onusseit, and F. Porsch, Liq. Cryst. **1**, 1 (1986).
[3] R.M. Hornreich and S. Shtrikman, Mol. Cryst. Liq. Cryst. **165**, 183 (1988).
[4] S.R. Renn and T.C. Lubensky, Phys. Rev. A **38**, 2132 (1988).
[5] J.W. Goodby, M.A. Waugh, S.M. Stein, E. Chin, R. Pindak, and J.S. Patel, Nature (London) **337**, 449 (1989).
[6] H.T. Nguyen, A. Bouchta, L. Navailles, P. Barois, N. Isaert, R.J. Twieg, A. Maaroufi, and C. Destrade, J. Phys. II **2**, 1889 (1992).
[7] L. Navailles, H.T. Nguyen, P. Barois, C. Destrade, and N. Isaert, Liq. Cryst. **15**, 479 (1993).
[8] L. Navailles, C.W. Garland, and H.T. Nguyen, J. Phys. II **6**, 1243 (1996).
[9] M.H. Li, H.T. Nguyen, and G. Sigaud, Liq. Cryst. **20**, 361 (1996).
[10] M.H. Li, V. Laux, H.T. Nguyen, G. Sigaud, P. Barois, and N. Isaert, Liq. Cryst. **23**, 389 (1997).
[11] M. Young, G. Pitsi, M.H. Li, H.T. Nguyen, P. Jamée, G. Sigaud, and I. Thoen, Liq. Cryst. **25**, 387 (1998).
[12] B. Pansu, M.H. Li, and H.T. Nguyen, J. Phys. II **7**, 751 (1997).
[13] B. Pansu, M.H. Li, and H.T. Nguyen, Eur. Phys. J. B **2**, 143 (1998).
[14] O. Onusseit and H. Stegemeyer, Liq. Cryst. **10**, 869 (1991).
[15] E. Demikhov, H. Stegemeyer, and V. Tsukruk, Phys. Rev. A **46**, 4879 (1992).
[16] E. Grelet, B. Pansu, and D. Dallé (unpublished).
[17] H.S. Kitzerow, Mol. Cryst. Liq. Cryst. **202**, 51 (1991).
[18] J. Englert, L. Longa, H. Stark, and H.R. Trebin, Phys. Rev. Lett. **81**, 1457 (1998).
[19] R. Kamien, J. Phys. II **7**, 765 (1997).
[20] R. Barbet-Massin, P.E. Cladis, and P. Pieranski, Phys. Rev. A **30**, 1161 (1984).